

## Two-color above-threshold and two-photon sequential double ionization beyond the dipole approximation

This content has been downloaded from IOPscience. Please scroll down to see the full text.

2015 J. Phys.: Conf. Ser. 601 012012

(<http://iopscience.iop.org/1742-6596/601/1/012012>)

View [the table of contents for this issue](#), or go to the [journal homepage](#) for more

Download details:

IP Address: 92.243.181.209

This content was downloaded on 22/04/2015 at 08:45

Please note that [terms and conditions apply](#).

# Two-color above-threshold and two-photon sequential double ionization beyond the dipole approximation

A N Grum-Grzhimailo<sup>1</sup>, E V Gryzlova<sup>1</sup>, E I Kuzmina<sup>1,2</sup>,  
A S Chetverkina<sup>1,2</sup> and S I Strakhova<sup>1</sup>

<sup>1</sup>Skobeltsyn Institute of Nuclear Physics, Lomonosov Moscow State University, Moscow 119991, Russia

<sup>2</sup>Faculty of Physics, Lomonosov Moscow State University, Moscow 119991, Russia

E-mail: algrgr1492@yahoo.com

**Abstract.** Two nonlinear atomic photoprocesses are theoretically considered with the emphasis on the photoelectron angular distributions and their modifications due to violation of the dipole approximation: sequential two-photon double ionization and two-color above threshold ionization. These reactions are now accessible with X-ray free electron lasers. Both processes are exemplified by the ionization of krypton: from the 4p shell in the sequential two-photon double ionization and from the 2s shell in the two-color above-threshold ionization, which are compared to the Ar(3p) and Ne(1s) ionization, respectively. Noticeable nondipole effects are predicted.

## 1. Introduction

Recent advances in development and use of free-electron lasers (FELs) producing very intense X-ray and VUV radiation made it possible to observe angular distributions of emitted electrons in non-linear atomic photoprocesses in this energy range (for example, [1, 2, 3, 4]). It is known that the photoelectron angular distributions (PADs) are sensitive to the interference between photoionization amplitudes of different multiplicity and parity and that this interference (dominantly between the electric dipole E1 and electric quadrupole E2 amplitudes) can influence the PAD in the one-photon single ionization already in the VUV region leading to pronounced non-dipole effects [5, 6, 7]. Naturally, the non-dipole effects should show up for non-linear photoprocesses in a similar energy range. Thus, motivated by the achievements in using the X-ray FELs, we have developed a theory for the PADs and angular correlations between the two emitted electrons in sequential two-photon double ionization (2PDI) [8] (figure 1a) and the PADs for two-color above-threshold ionization (ATI) [9] of atoms (figure 1b) beyond the dipole approximation. In the latter case, the XUV photon generates the nondipole transitions to the atomic continuum which are then monitored by the optical (IR) radiation.

Numerical predictions for the non-dipole effects were made for the 2PDI of the outer  $np^6$  shells of neon and argon by linearly polarized radiation [8, 10] and of neon, argon and krypton for circularly polarized radiation [11]. In section 2 of this contribution we 'fill the gap' and present the results for the 2PDI of the  $4p^6$  shell in krypton by linearly polarized FEL. An extra Cooper minimum in the quadrupole cross section leads to differences in the general behavior of PADs in sequential 2PDI of Kr and Ar from 4p and 3p shells, respectively. In section 3 we give



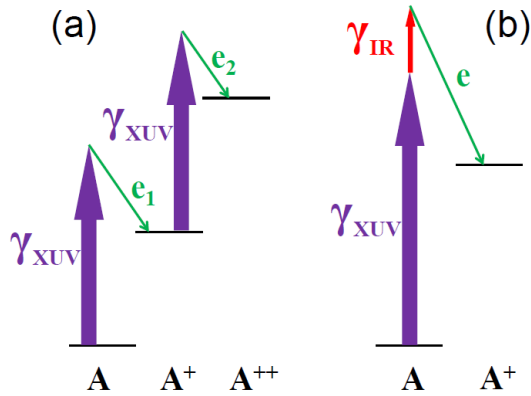


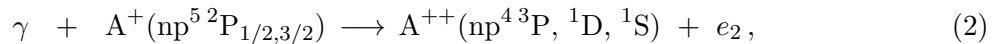
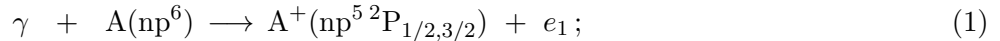
**Figure 1.** Schemes of sequential 2PDI (a) and two-color ATI (b).

predictions for the two-color XUV + optical laser ATI of the 2s shell in atomic Kr and compare the results with the similar process for the 1s ionization in atomic Ne.

We assume that the photon pulses contain many optical cycles and that the photon beams are either mutually incoherent (in the two-color ATI) or the coherence is lost between the two steps of the process (2PDI). Under these conditions, the effects of the pulse shape, relative phase of the electromagnetic fields and other effects for which the time dependence of the electromagnetic field is crucial, are irrelevant in treatment of the PADs. Furthermore, in the lowest order perturbation theory, the PADs are independent of the beam intensities.

## 2. Sequential two-photon double ionization

The PADs in the sequential 2PDI were studied, both experimentally and theoretically, mostly for the outer shells of the noble gases. In a stepwise approximation this reaction proceeds in two steps,



with possible evolution of the polarized intermediate ion  $A^+(np^5 2P_{1/2,3/2})$  between the two steps. Electrons  $e_1$  and  $e_2$  are well distinguished by their kinetic energy. Expressions for the angular distributions and correlations of the emitted electrons  $e_1$  and  $e_2$  in the sequential 2PDI have been obtained in [8] within the statistical tensor formalism taking into account the full multipole expansion of radiation in electric and magnetic moments. The formalism was further specified for linearly polarized [8] and circularly polarized [11] FEL beams with inclusion of the first-order corrections to the dipole approximation due to the E1-E2 interference of the multipole amplitudes.

We concentrate here on the PAD of the second electron  $e_2$ . For a linearly polarized FEL beam it is of the form

$$\begin{aligned} \frac{d\sigma}{d\Omega} = & \frac{\sigma}{4\pi} \left( 1 + \beta_2^{(2)} P_2(\cos \vartheta) + \beta_4^{(2)} P_4(\cos \vartheta) \right. \\ & \left. + \left( \delta^{(2)} + \gamma_2^{(2)} \cos^2 \vartheta + \gamma_4^{(2)} \cos^4 \vartheta \right) \sin \vartheta \cos \varphi \right), \end{aligned} \quad (3)$$

where  $\sigma$  is the angle integrated ionization cross section in the dipole approximation (the E1-E2 interference terms vanish in the angle integrated cross section), the z-axis of the coordinate system is directed along the electric field (polarization vector) of the FEL beam, which propagates along the x-axis. The first three terms and the asymmetry parameters  $\beta_2^{(2)}$ ,  $\beta_4^{(2)}$

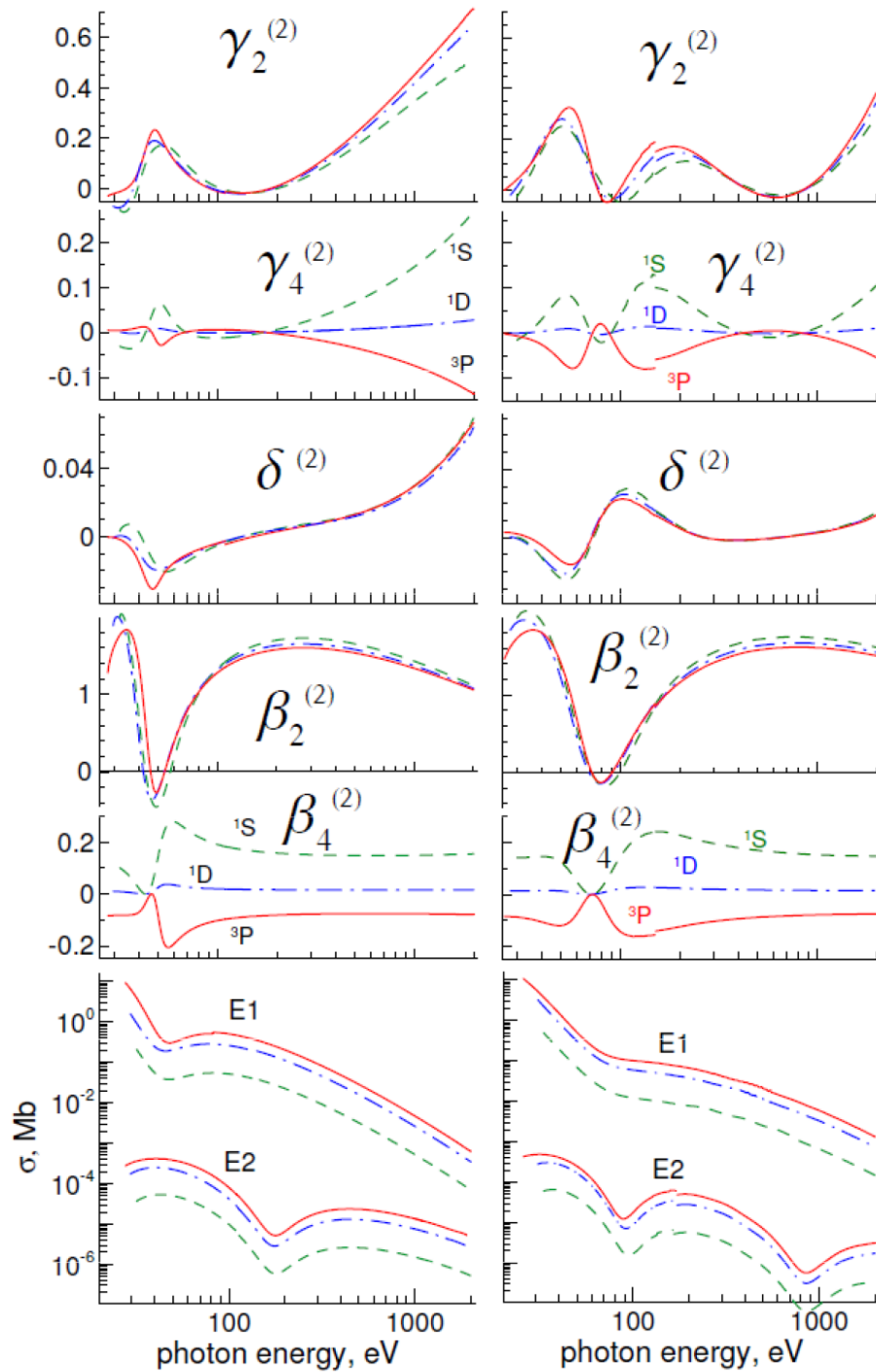


**Figure 2.** Dipole (E1) and quadrupole (E2) cross sections (bottom panels) and asymmetry parameters of the PAD (3) emitted in sequential 2PDI of the valence  $3p^6$  shell of Ar (left column) and  $4p^6$  shell of Kr (right column) for different  $LS$  terms of the residual doubly charged ion  $A^{++}(np^4)$  as a function of the photon energy:  $^3P$  (solid red),  $^1D$  (chain blue),  $^1S$  (dashed green). See text for an explanation of the discontinuity in some curves for Kr at about 150 eV.

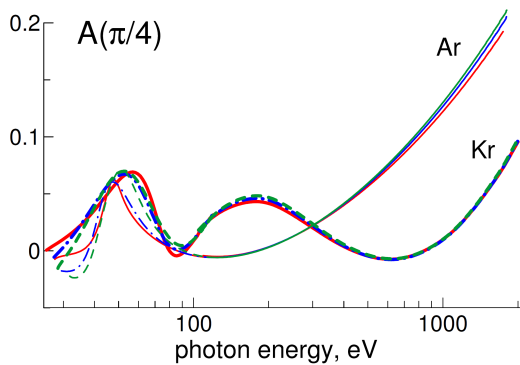


**Figure 3.** Differential forward-backward asymmetry (4) for  $\vartheta = \frac{\pi}{4}$  as a function of the photon energy for different final multiplet states of  $\text{Kr}^{++}(4p^4)$  (bold lines) and  $\text{Ar}^{++}(3p^4)$  (thin lines) at 2PDI. Curves as in figure 2.

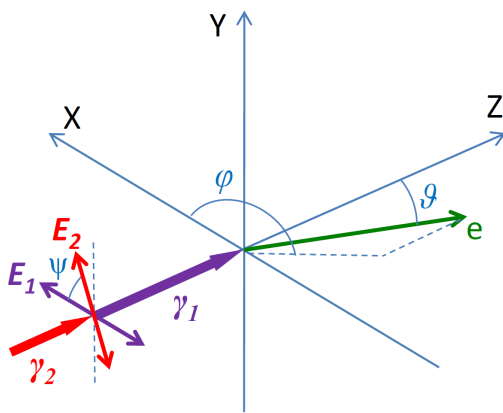


**Figure 4.** Geometry of the two-color ATI by two parallel linearly polarized radiation beams  $\gamma_1$  and  $\gamma_2$ . Vectors  $\mathbf{E}_1$  and  $\mathbf{E}_2$  denote the corresponding directions of the linear polarization.

correspond to the pure dipole contribution; the last three terms with the parameters  $\delta^{(2)}$ ,  $\gamma_2^{(2)}$ ,  $\gamma_4^{(2)}$  give the first-order non-dipole corrections and appear due to the E1-E2 interference.

The asymmetry parameters in equation (3) are expressed in terms of the photoionization amplitudes [8]. The atomic model used in the calculations of the matrix elements is based on the multiconfiguration Hartree-Fock (MCHF) approach and has been described for Kr in [12]. Excitation of the intermediate  $\text{Kr}^+ 4p^5 {}^2P_{1/2,3/2}$  fine-structure ionic states is treated as incoherent and the corresponding contributions to the cross sections and PADs are summed up, as well as the contributions from unresolved fine-structure states of the final doubly charged ion  $\text{Kr}^{++} 4p^4 {}^3P_{0,1,2}$ . The intermediate ionic spin-orbit doublets of  $\text{Ar}^+(3p^5)$ , and  $\text{Kr}^+(4p^5)$  are splitted by 0.177 eV, and 0.656 eV, respectively. As it was confirmed by calculations of Nikolopoulos [13], the time parameter defining the coherency of the excitation is the spin-orbit precession time: 23.30 fs for  $\text{Ar}^+$ , and 6.21 fs for  $\text{Kr}^+$ . Thus for Kr, the excitation can be treated as incoherent for almost all pulses currently generated by FELs in the XUV.

The five upper double panels of figure 2 show the asymmetry parameters in equation (3) for the sequential 2PDI of the argon 3p and krypton 4p shell. The bottom panels display the corresponding angle integrated dipole (E1) and quadrupole (E2) ionization cross sections. The results for Ar [10] are shown for comparison and the scales of the corresponding plots for Ar and Kr are identical. For high enough photon energies, the difference between the MCHF and single-configuration calculations becomes negligible. For these energies we used therefore the single-configuration model, which provides better stability in calculations of the continuum wavefunctions. This explains the tiny jumps in some curves for Kr in figure 2 at about 150 eV.

The pure dipole parameters  $\beta_2^{(2)}$  and  $\beta_4^{(2)}$  for Ar and Kr qualitatively behave similar as functions of the photon energy. The Cooper minimum in the dipole  $np \rightarrow Ed$  amplitude is the

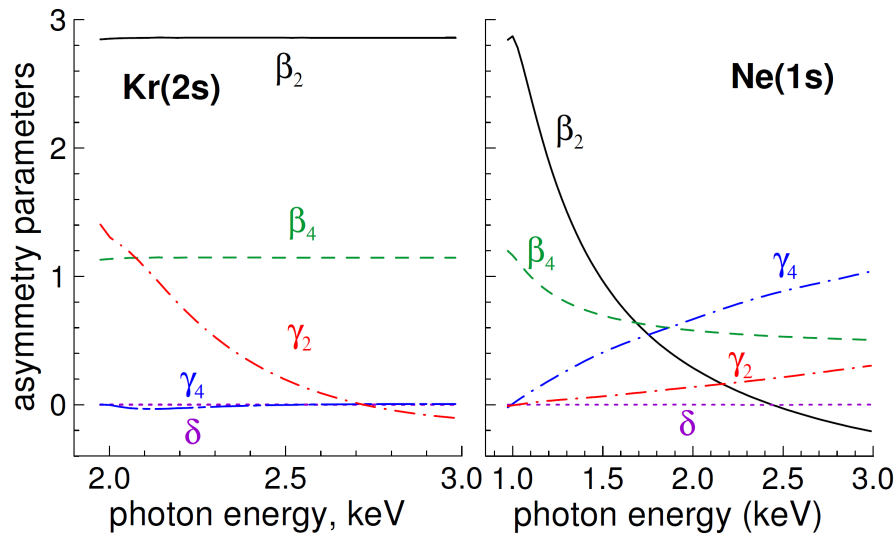


**Figure 5.** Angular asymmetry parameters of equation (3) for the two-color Kr(2s) (left) and Ne(1s) (right) ATI by linearly polarized in the same direction photons.

reason for sharp changes in the parameters. This minimum, seen in the E1 curves for the cross sections, is filled due to the  $np \rightarrow E_s$  ionization transitions. As has been discussed in detailed in [10] for the case of Ar, the decrease of the dipole ionization causes an increase of the non-dipole asymmetry parameters. In contrary, the Cooper minima in the quadrupole  $np \rightarrow E_f$  amplitude, located around 200 eV photon energy for  $Ar^+$  and around 100 eV and 800 eV for  $Kr^+$ , lead to negligible values of  $\delta^{(2)}$ ,  $\gamma_2^{(2)}$ ,  $\gamma_4^{(2)}$  in these regions. The two quadrupole Cooper minima in  $Kr^+$  against the single one in  $Ar^+$  cause differences in the energy dependence of the nondipole asymmetry parameters for these two atoms: while in Ar the absolute values of the parameters increase monotonically with photon energy starting from 200 eV, the parameters in Kr show a second minimum at higher energies.

Similar features are demonstrated in figure 3 for the differential forward-backward asymmetry (in the  $xz$  plane)

$$A(\vartheta) = \left[ \frac{d\sigma}{d\Omega}(\vartheta) - \frac{d\sigma}{d\Omega}(\pi - \vartheta) \right] / \left[ \frac{d\sigma}{d\Omega}(\vartheta) + \frac{d\sigma}{d\Omega}(\pi - \vartheta) \right] \quad (4)$$

for  $\vartheta = \frac{\pi}{4}$ . The forward-backward asymmetry is a convenient quantity to study nondipole effects, since it vanishes in the dipole approximation. Noteworthy, the asymmetries (4) for sequential 2PDI in both Ar and Kr are similar for  $np^4 \ ^3P$ ,  $^1D$ , and  $^1S$  final states, except near the threshold. Therefore it is experimentally not required to resolve these multiplet states by the electron spectrometer for high electron energies, where the nondipole effects are generally larger. At the same time, an asymmetry of more than 5% is predicted for both Ar and Kr at low photon energies of 50–60 eV in the region of the Cooper minimum for the  $np \rightarrow E_d$  transition.

The non-dipole effects notably change the PADs. In the Cooper minimum for the  $np$  ionization of  $Ar^+$  and  $Kr^+$  at photon energies of tens of eV, the predicted non-dipole effects are as pronounced as at photon energies of about 1 keV, but the conditions of their observation are better in the Cooper minimum due to the much larger photoionization cross sections at lower photon energies [10].

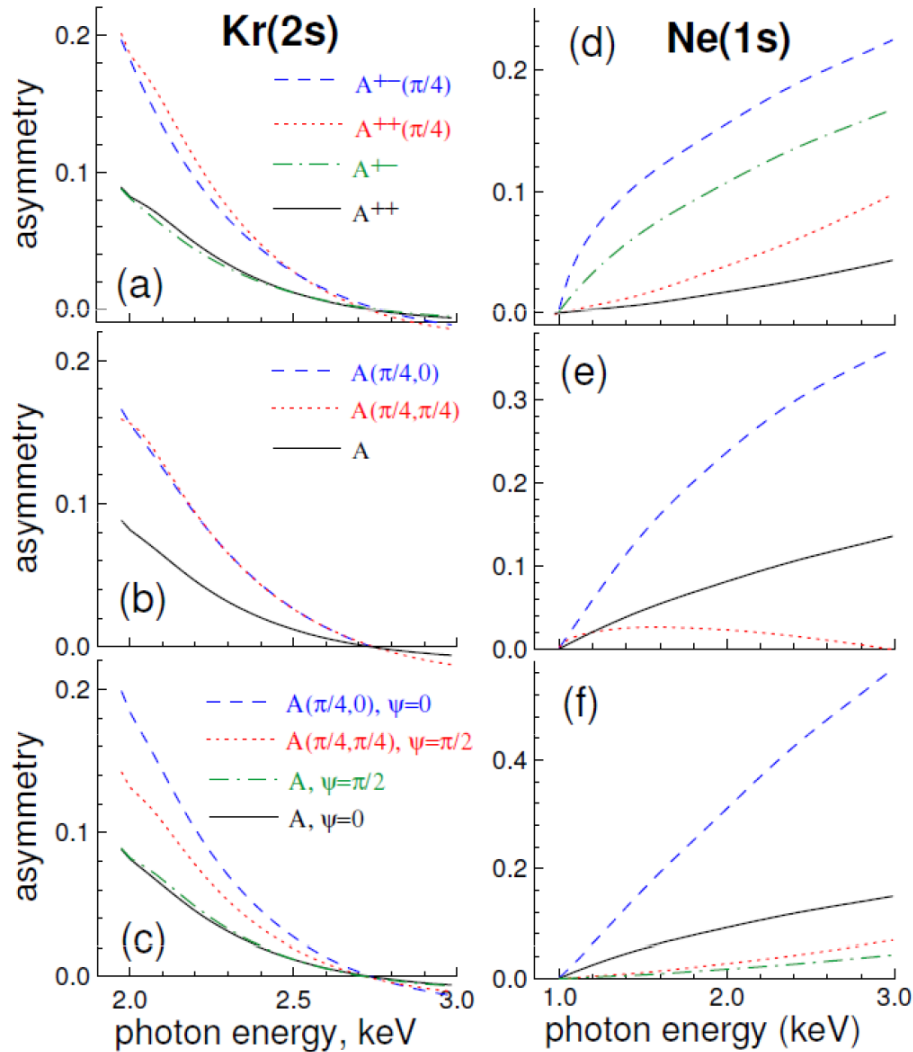


**Figure 6.** Forward-backward differential asymmetries  $A(\vartheta, \varphi)$  (4), and integral asymmetries  $A$  (5), for circularly polarized XUV and IR photons (a) and (d), linearly polarized XUV photon and circularly polarized IR photon (b) and (e), and linearly polarized XUV and IR photons (c) and (f). Left column: for Kr(2s) ATI; right column: for Ne(1s) ATI.

### 3. Two-color above-threshold ionization

Here we apply the formalism for the PADs in two-color ATI to the experimentally most feasible arrangement with collinear photon beams and emphasize independently variable polarizations of the radiation beams [9]. The geometry for two linearly polarized beams is shown in figure 4. Particular expressions for the PADs within the first-order non-dipole corrections have been derived in [9]. In particular, for parallel polarizations ( $\psi = 0$ ), the PAD in the ATI line is described by an equation similar to (3). To avoid confusion, for the ATI (i.e. single ionization) we will use another notations for the asymmetry parameters in (3):  $\beta_2^{(2)} \rightarrow \beta_2$ ,  $\beta_4^{(2)} \rightarrow \beta_4$ ,  $\delta^{(2)} \rightarrow \delta$ ,  $\gamma_2^{(2)} \rightarrow \gamma_2$ ,  $\gamma_4^{(2)} \rightarrow \gamma_4$ .

Numerical results for the amplitudes of the two-color Kr(2s) ATI were obtained here within the second-order perturbation theory similar to the treatment of Ne(1s) in [9]. The energy of the optical photon was fixed at 1.5 eV. The ionization thresholds of the 2s shell in Kr and of

the 1s shell in Ne are 1923 eV and 870 eV, respectively. It is known from the calculations [6] that the nondipole effects in the PAD for the single-photon Kr(2s) ionization are large close to the ionization threshold and with increasing photon energy they are first decreasing. The latter feature is not usual, since normally the relative contribution of the higher multipoles of the radiation increases with increasing photon energy leading also to the increasing non-dipole effects (like in the Ne(1s) ionization [6]). Figure 5 shows that similar counter trends persist in the two-color Kr(2s) and Ne(1s) ATI: the nondipole parameter  $\gamma_2$  is decreasing for Kr(2s), while the nondipole parameters  $\gamma_2$  and  $\gamma_4$  are increasing for Ne(1s). The calculations reveal another interesting feature of the dipole parameters  $\beta_2$  and  $\beta_4$ : they strongly vary with photon energy for the Ne(1s) ATI and are nearly constants for the Kr(2s) ATI. Our analysis shows that the nearly constant values of the parameters  $\beta_2$  and  $\beta_4$  follow from the dynamical calculations for the Kr(2s) ATI and are related to an 'accidentally' almost constant absolute ratio of the Es and Ed two-photon ionization amplitudes in the broad range of photon energies. This feature is supposed to be model-dependent.

The differential forward-backward asymmetry (4) for the case of one circular and one linear polarized beam depends on the azimuthal angle  $\varphi$ ,  $A = A(\vartheta, \varphi)$ . For two linearly polarized beams, the asymmetry depends additionally on the adjustable angle  $\psi$  between the polarization directions of the photon beams (see figure 4). The integral forward-backward asymmetry is defined as

$$A = \frac{\sigma_{\Omega+} - \sigma_{\Omega-}}{\sigma_{\Omega+} + \sigma_{\Omega-}}, \quad (5)$$

where  $\sigma_{\Omega+}$  ( $\sigma_{\Omega-}$ ) is the photoelectron flux integrated over the forward (backward) hemisphere. Figure 6 shows various types of forward-backward asymmetry as function of the photon energy. Comparing the Kr(2s) and Ne(1s) ATI, it is clearly seen that, again, all asymmetries for Kr(2s) are maximal at the ionization threshold and drop down with increasing photon energy, while the asymmetries for Ne(1s) are negligible at the ionization threshold and increase with increasing photon energy. At the photon energies considered here, the asymmetries for Kr(2s) are not larger than 0.2, which is smaller than some of the asymmetries for Ne(1s) (figure 6).

#### 4. Conclusion

We predicted noticeable nondipole effects in two-photon two-color above-threshold Kr(2s) ionization and in sequential two-photon Kr(4p) double ionization. Some new features of the processes are predicted in comparison with the Ne(1s) and Ar(3p) ionization, respectively. The non-dipole effects can be observed with existing FEL facilities and combining XUV FEL and optical laser beams. We hope that the results presented will stimulate experiments on non-dipole effects in nonlinear atomic photoprocesses.

#### Acknowledgments

The authors acknowledge support by the Russian Foundation for Basic Research (RFBR) under Grant No. 12-02-01123. EVG gratefully acknowledges financial support by the Dynasty Foundation via the Support Program for Young Scientists. Fruitful discussions with Dr Michael Meyer are gratefully acknowledged.

#### References

- [1] Berrah N *et al* 2010 *J. Mod. Opt.* **57** 1015
- [2] Bostedt C *et al* 2013 *J. Phys. B: At. Mol. Opt. Phys.* **46** 164003
- [3] Feldhaus J *et al* 2013 *J. Phys. B: At. Mol. Opt. Phys.* **46** 164002
- [4] Yabashi M *et al* 2013 *J. Phys. B: At. Mol. Opt. Phys.* **46** 164001
- [5] Guillemin R, Hemmers O, Lindle D W and Manson S T 2006 *Radiat. Phys. Chem.* **75** 2258
- [6] Trzhaskovskaya M B, Nefedov V I and Yarzhevsky V G 2001 *Atomic Data and Nuclear Data Tables* **77** 97

- [7] Kleinpoppen H, Lohmann B and Grum-Grzhimailo A N 2013 *Perfect/Complete Scattering Experiments* (Berlin: Springer) p 283
- [8] Grum-Grzhimailo A N, Gryzlova E V and Meyer M 2012 *J. Phys. B: At. Mol. Opt. Phys.* **45** 215602
- [9] Grum-Grzhimailo A N and Gryzlova E V 2014 *Phys. Rev. A* **89** 043424
- [10] Gryzlova E V, Grum-Grzhimailo A N, Strakhova S I and Meyer M 2013 *J. Phys. B: At. Mol. Opt. Phys.* **46** 164014
- [11] Gryzlova E V, Grum-Grzhimailo A N, Kuzmina E I and Strakhova S I 2014 *J. Phys. B: At. Mol. Opt. Phys.* **47** 195601
- [12] Fritzsche S, Grum-Grzhimailo A N, Gryzlova E V and Kabachnik N M 2009 *J. Phys. B: At. Mol. Opt. Phys.* **42** 145602
- [13] Nikolopoulos L A A 2013 *Phys. Rev. Lett.* **111** 093001